catalysts

MDPI

Article

A Case Study for the Deactivation and Regeneration of a V_2O_5-WO_3/TiO_2 Catalyst in a Tail-End SCR Unit of a Municipal Waste Incineration Plant

Stefano Cimino [1,*], Claudio Ferone [2], Raffaele Cioffi [2], Giovanni Perillo [3] and Luciana Lisi [1,*]

1 Istituto Ricerche sulla Combustione, CNR, 80125 Napoli, Italy
2 Department of Engineering, University Parthenope of Napoli, 80143 Napoli, Italy; claudio.ferone@uniparthenope.it (C.F.); raffaele.cioffi@uniparthenope.it (R.C.)
3 Wessex Institute of Technology, Southampton SO40 7AA, UK; giovanni.perillo@uniparthenope.it
* Correspondence: stefano.cimino@cnr.it (S.C.); l.lisi@irc.cnr.it (L.L.)

Received: 5 May 2019; Accepted: 15 May 2019; Published: 20 May 2019

Abstract: In this work, we set out to investigate the deactivation of a commercial V_2O_5-WO_3/TiO_2 monolith catalyst that operated for a total of 18,000 h in a selective catalytic reduction unit treating the exhaust gases of a municipal waste incinerator in a tail end configuration. Extensive physical and chemical characterization analyses were performed comparing results for fresh and aged catalyst samples. The nature of poisoning species was determined with regards to their impact on the DeNOx catalytic activity which was experimentally evaluated through catalytic tests in the temperature range 90–500 °C at a gas hourly space velocity of 100,000 h^{-1} (NO = NH_3 = 400 ppmv, 6% O_2). Two simple regeneration strategies were also investigated: thermal treatment under static air at 400–450 °C and water washing at room temperature. The effectiveness of each treatment was determined on the basis of its ability to remove specific poisoning compounds and to restore the original performance of the virgin catalyst.

Keywords: DeNOx; MW incinerator; deactivation; ammonium sulfates; regeneration; washing

1. Introduction

Selective catalytic reduction (SCR) of nitrogen oxides with ammonia is one of the most widely used technologies for reducing NOx from both stationary and mobile sources [1,2]. This technology and, in particular, its application to the exhaust of fossil fuel-fired power plants, is quite mature. Nevertheless, more recent applications to industrial and municipal waste (MW) incinerators pose new issues related to the heterogeneity and variability of the fuel with the consequent release of different pollutants which have to be suitably treated before emission to the atmosphere [3,4]. In addition to SO_x, CO, and particulate matter, exhaust gases deriving from the combustion of solid wastes contain large amounts of alkali and alkaline-earth metals (potassium, sodium, calcium, magnesium), phosphorous, and chlorine [4]. All these pollutants must be controlled within the limit values defined by the more and more stringent environmental regulations.

Catalysts for the SCR of NOx in exhaust gases from MW incinerator are generally of the same type employed in traditional power plants, namely V_2O_5-WO_3/TiO_2. Poisoning/deactivation of such catalysts during operation with the exhaust gases from coal-fired plants has been widely investigated, mainly concerning compounds such as SO_2, mercury, arsenic, alkaline, and alkaline earth oxides [4]. Under conventional operating conditions, the expected catalyst lifetime has been well defined and possible regeneration strategies proposed, as catalysts represent the main cost of the SCR process [2,5]. More recently, research has been extended to poisoning of SCR catalysts for NOx abatement in flue

gases from MW and biomass combustion [3–7]. The SCR unit in a MW incinerator plant is possibly located just after the boiler as high dust system where temperatures are high enough (300–400 °C) to assure optimal catalytic performance. In this configuration, however, SO_2, fly ashes, acid gases and particulate, not yet removed, impact the SCR catalyst. In addition, alkali and alkaline-earth metals, mostly present into the ashes which are more abundant in the MW emissions, can further deactivate the catalyst strongly reducing its lifetime [4–7].

In general, alkali and alkaline-earth metals deactivate the catalyst reducing the number of acid sites [8–11]. Nevertheless, one of the major causes of poisoning, also for MW incineration, remains the formation of ammonium sulfate and bi-sulfate on the catalyst surface mostly when the operation temperature is below 290 °C [5,11] due to the reaction occurring between ammonia and SO_3 produced by SO_2 oxidation. In particular, sulfates poisoning can reduce surface area and porosity by pore clogging or can affect the surface acidity [11–13]. Kröcher and Elesener [13] reported that potassium reacted with vanadium forming potassium vanadate whereas calcium sulfate just physically masks the active sites forming a barrier layer. Nicosia et al. [10] also investigated the deactivating effect of K and Ca on traditional SCR catalysts which affected both Brønsted and Lewis acidity of V_2O_5 inhibiting both the NH_3 adsorption and the decomposition of the nitrosamide intermediate. The extent of deactivation also depends on the counterion of the alkali or alkaline-earth metal cation [14]. It was reported [10] that calcium causes a strong reduction of activity if coupled with an organic anion whilst the deactivation is almost negligible when anions from inorganic acid are present on the surface. Among its inorganic salts, calcium deactivates the SCR catalyst in the following order: $SO_4^{2-} > PO_4^{3-} > BO^{3-}$ [12].

The tail-end configuration of the SCR unit is less common. It involves gas re-heating due to the complex upstream system of emissions control with additional costs related to the fuel to increase the gas temperature up to 180–250 °C [5]. Nevertheless, the tail-end arrangement enables the use of a high-activity catalyst with small diameter channels, since particulates and SO_2 have already been removed upstream; moreover, the expected deactivation rate is low due to the absence of fly ash and other poisons so that catalyst life is substantially extended [5].

In this paper, we report a case study on the deactivation of a commercial V_2O_5-WO_3/TiO_2 monolith catalyst operated for 18,000 h in a SCR (DeNOx) unit with tail-end configuration treating the exhaust gases of a MW incinerator plant located in Southern Italy [15]. The SCR unit, operating with ammonia injection at around 200 °C, is placed downstream a purification train consisting of dry and semi-dry absorbers with lime and active carbon injection to remove HCl, HF, SO_x; active carbon adsorber to remove heavy metals and organo-chlorinated compounds; bag filters to eliminate particulate matter [15]. The possible deactivating mechanisms and poisoning compounds were identified by several characterization techniques trying to establish their origin; the extent of deactivation was estimated by kinetic measurements of the SCR catalytic activity. Simple regeneration strategies such as thermal treatments in air and washing in water were investigated on the basis of the results of chemical and physical characterization of the aged catalyst.

2. Results

The commercial SCR catalyst consisted of a V_2O_5-WO_3/TiO_2 honeycomb monolith sample with square channels, a cell density of 7.3 cell/cm^2, and an overall density of 500 g/dm^3. Glass fibers with a characteristic diameter around 10 μm were distributed in the bulk of the material to provide mechanical resistance to the extruded monolith.

XRF analysis of virgin monolith catalyst indicated that the loading of the two active metals (V and W) was 3.51% and 6.36% when expressed as oxides respectively (Table 1), which is typical of SCR catalysts for stationary applications [1,16]. SEM-EDS analysis of fresh monolith sample (not shown) indicated that vanadium, tungsten, and titanium were uniformly distributed, whereas the silica content was associated with the reinforcing glass fibers. The catalyst also contained small amounts of iron and sulfur (Table 1), which are generally added to enhance the catalytic performance [17–19].

Table 1. Chemical composition of the fresh catalyst by XRF analysis.

	TiO_2	WO_3	V_2O_5	SiO_2	Al_2O_3	CaO	Fe_2O_3	SO_4^{--}
%wt	85.53	6.36	3.51	2.01	1.10	1.14	0.30	0.38

The fresh monolith had a surface area of ca. 54 m^2/g (Table 2) that falls in the typical range of values (50–60 m^2/g) generally reported for commercial mesoporous TiO_2 in the anatase phase. In fact, XRD analysis (not shown) confirmed the presence of a pure TiO_2 anatase phase. Moreover, the results of pore size distribution (PSD) analysis reported in Figure 1 revealed the presence of mesopores with characteristic diameters in the range 60–300 Å.

Table 2. BET surface area and volume of pores of fresh, aged and regenerated selective catalytic reduction (SCR) catalysts.

Sample	Pre-Treatment	BET s.a. m^2/g	V cc/g
Fresh catalyst		53.8	0.25
Aged 18 kh		43.4	0.26
Regen. R400	2 h @400 °C	44.8	0.26
Regen. R450	2 h @450 °C	44.8	0.26
Regen. WW	30 min in water	48.4	0.30

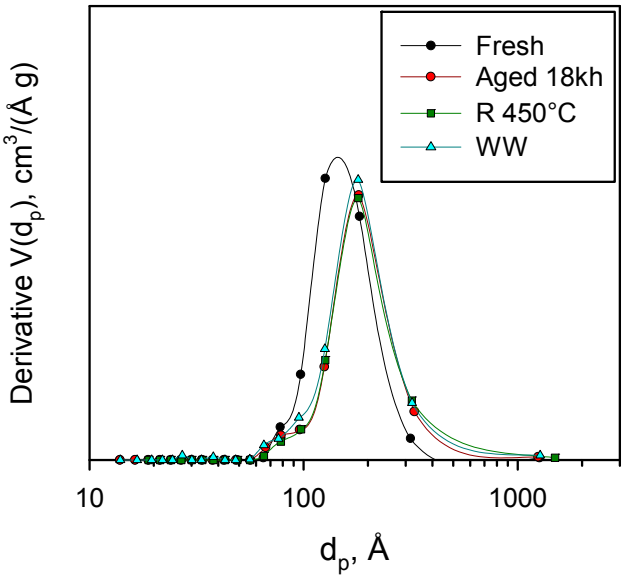

Figure 1. Pore size distribution for fresh, aged, and regenerated catalysts by heat treatment (R 450 °C) or washed in water (WW).

After 18 kh of operation, the BET specific surface area of the aged catalyst dropped by ca. 20% down to 43 m^2/g without any significant change in the total pore volume (Table 2), suggesting an increase of the average pore size. In fact, the PSD analysis indicates the partial loss of those mesopores in the range 80–170 Å (Figure 1), possibly due to occlusion and/or collapse.

The typical yellowish color of the virgin SCR catalyst turned into grey after 18 kh on stream, with some brownish shades in correspondence to the inlet edge the monolith (Figure 2a,b). However, the cross-section of the honeycomb channels was free due to the absence of massive ash deposition and to a rather limited occurrence of erosion phenomena (Figure 2a).

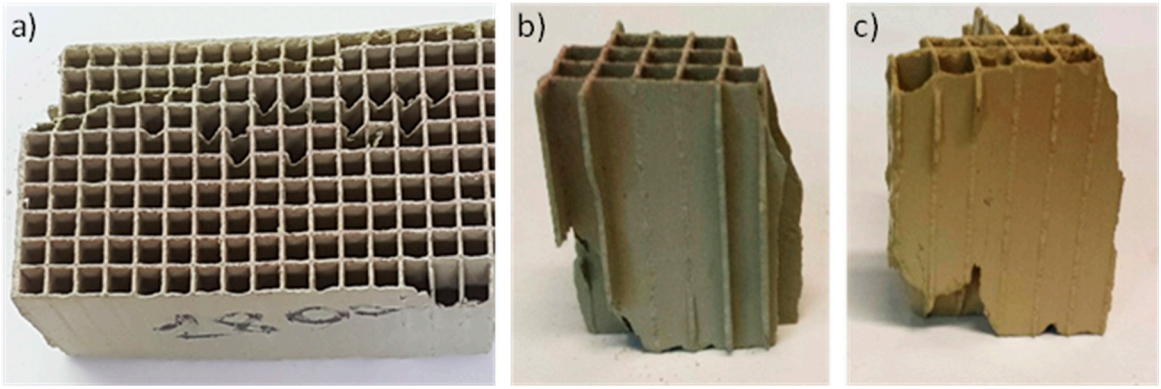

Figure 2. Appearance of the reaction-aged (18 kh) SCR honeycomb catalyst ((**a**,**b**): samples taken from the inlet section of the monolith) in comparison with a sample of the same catalyst after regeneration by washing in water (**c**).

SEM with EDS elemental analysis was performed at three different positions along the monolith channel close to the inlet section (1, 5, 10 mm from it) selecting two areas of 271 × 271 μm for each position; Table 3 reports the corresponding results for the elemental concentration of S and Ca.

Table 3. EDS elemental analysis of the surface concentration of sulfur and calcium at different locations along the channel of the reaction-aged SCR catalytic honeycomb (distance from inlet: a, a′ = 1 mm; b, b′ = 5 mm; c, c′ = 10 mm).

Location Along the Monolith		**a**	**a′**	**b**	**b′**	**c**	**c′**
Distance from inlet	[mm]	1		5		10	
Sulfur	[wt%]	4.3	2.6	2.2	2.3	1.3	1.1
Calcium	[wt%]	2.9	1.4	0.5	0.2	0.2	0.5
S/Ca	atomic	1.9	2.3	5.5	14.4	8.1	2.8

Calcium and sulfur were detected at relatively high concentrations close to the monolith inlet but their amount decreased along the channel length. This is better highlighted in Figure 3, where the elemental distribution is shown for zones a and b (Table 3). The overlapping of the most intense spots associated with sulfur and calcium confirms that indeed they were associated with the presence of $CaSO_4$ deposits. The additional formation of other sulfate species can be inferred by the higher atomic concentration of sulfur with respect to calcium detected in all investigated areas (Table 3).

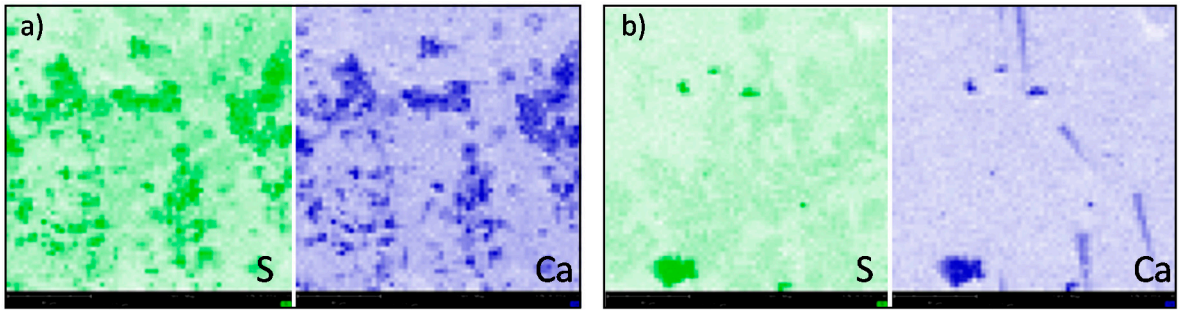

Figure 3. Sulfur (**green**) and calcium (**blue**) distribution maps at two locations ((**a**): 0.1 cm and (**b**): 0.5 cm from inlet) along a central channel of the 18 kh reaction-aged SCR honeycomb catalyst.

The larger content of calcium in the aged catalyst was most likely due to the dragging of fine particles from the upstream fabric filters that follow a desulfurization unit based on the injection of

hydrated lime [15]. Notably, the presence of $CaSO_4$ surface deposits can derive directly from dragging of $CaSO_4$ powders or by the reaction of $Ca(OH)_2$, which is preferentially deposited where sulfur is present at a higher level.

The surface acid properties of the fresh monolith catalyst were evaluated by performing NH_3 temperature programmed desorption (TPD) runs after saturating the sample with ammonia at 100 °C. The corresponding TPD profile, reported in Figure 4, is quite broad and it is the result of the overlap of at least two peaks. Ammonia desorption starts from the adsorption temperature (100 °C) and ends at about 470 °C indicating a wide distribution of acid sites with different strengths, which can be assigned to the anatase TiO_2 support [13]. By integration of the TPD curve, the total amount of NH_3 was calculated to equal 0.161 mmol/g, which agrees well with values reported for other commercial SCR catalysts taking into account the different exposed surface areas [8].

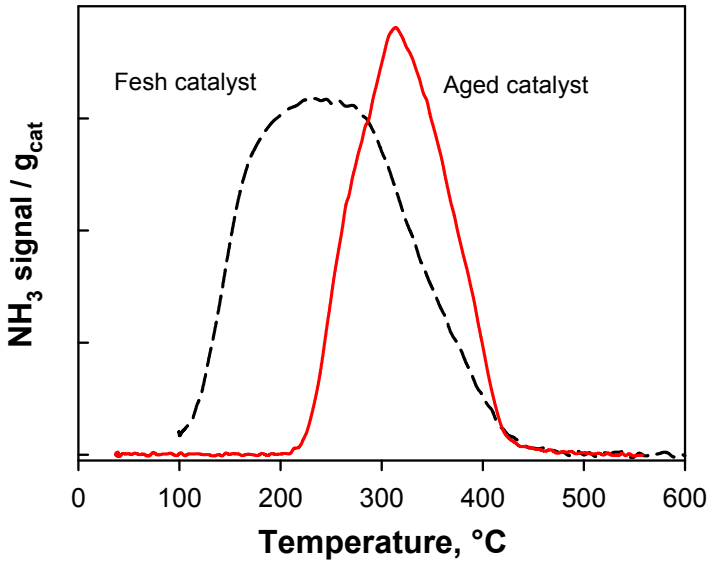

Figure 4. NH_3 temperature programmed desorption (TPD) of fresh and aged catalyst.

The NH_3 TPD of the aged sample carried out without pre-adsorbing ammonia at 100 °C (Figure 4), shows a more intense signal starting at about 210 °C, with a peak at 315 °C, and ending at the same temperature observed for the fresh catalyst. The ammonia adsorbed on the aged catalyst derived from its operation in the SCR reactor. Therefore, from the onset temperature of desorption, it can be argued that the last temperature the catalyst experienced in the SCR reactor was around 210 °C. The total amount of desorbed ammonia was lower (0.075 mmol/g) than the amount desorbed from the fresh sample due to the lack of NH_3 pre-adsorption step at 100 °C. Nevertheless, in the high-temperature range (above 300 °C), the NH_3 desorption peak for the aged catalyst exceeded that of the fresh catalyst. This result strongly suggests the decomposition of ammonium salts, like sulfate and bisulfate, probably formed by the reaction between NH_3 and SO_2/SO_3 or other superficial sulfates which were eventually deposited on the catalyst surface due to the low temperature of operation [7,11,18,20–22]. Notably, the content of gaseous SO_2 in the exhaust gas after the desulfurization unit is quite low (in the single digit ppmv range) [15].

The content of sulfates possibly adsorbed during the SCR operation was estimated by carrying out SO_2 TPD experiments under N_2 flow up to 900 °C on the aged catalyst in comparison with its fresh counterpart (Figure 5). Judging from its TPD trace it was confirmed that the virgin monolith contained some sulfur (see Table 1), likely in the form of sulfate species deliberately added during catalyst preparation in order to promote the SCR activity by increasing the number of acid sites for NH_3 adsorption [17]. By comparison with the TPD results of reference sulfate compounds, the SO_2 peaks between 400 and 600 °C were associated with the decomposition of sulfate species bonded to

titania and of $VOSO_4$ species [20,23], while the decomposition of iron sulfates might contribute at higher temperatures [24].

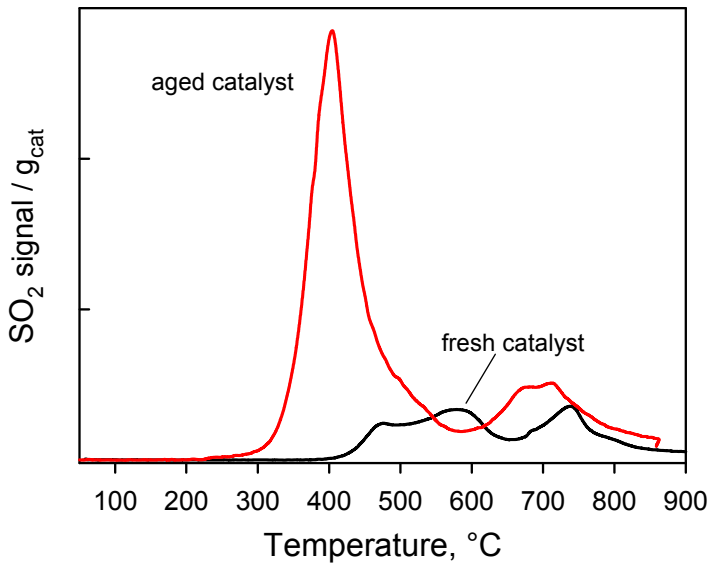

Figure 5. Comparison of SO_2 TPD for the fresh and 18 kh reaction-aged catalyst.

The onset temperature for SO_2 release from the virgin catalyst (400 °C) was a probable indication of the calcination temperature adopted during the preparation of the catalytic monoliths.

On the contrary, the reaction-aged catalyst showed an intense SO_2 desorption peak at low temperature starting from ca. 250 °C, which agrees with the accumulation of sulfates on the catalyst surface during operation. In fact, such a relatively low decomposition temperature is generally associated with the presence of ammonium (bi) sulfate [20], thus supporting the interpretation of the results from the NH_3 TPD test. However, when comparing the NH_3 and SO_2 desorption profiles from the aged catalyst it can be noticed that ammonia was released at a lower temperature with respect to SO_2 (Figures 4 and 5).

2.1. Regeneration Treatments

According to the characterization results of the reaction-aged catalyst, indicating the formation of ammonium sulfate and the deposition of $CaSO_4$ as the main possible causes of catalyst deactivation, two different types of regeneration treatments were investigated: (i) thermal treatment at 400 °C or 450 °C in static air; (ii) washing in (distilled) water at room temperature and subsequent drying. As mentioned before, the aged sample appeared grey in color in contrast to the green-yellowish fresh sample. Following both types of regeneration treatments, the original color was restored, as shown in Figure 2 for the case of water washed sample of the aged monolith.

Thermal regeneration of the aged catalyst at either 400 or 450 °C in air provided only limited recovery of the original surface area up to 45 m^2/g (Table 2). This is possibly caused by the volatilization/decomposition of some species formed and/or condensed on the catalyst during prolonged SCR operation. Nevertheless, the pore size distribution did not significantly change with respect to the aged catalyst (Figure 1), suggesting that the smallest mesopores were still partially blocked by relatively stable nano-particles or they were collapsed.

Washing in water was somehow more effective in restoring the surface area of the aged catalyst up to roughly 48 m^2/g (Table 2), though it also apparently increased the total pore volume, possibly due to the partial dissolution of some catalyst components. Notably, by washing the aged monolith in water it was possible to induce leaching of soluble species such as ammonium (bi) sulfate as well as the detachment of small debris and ashes largely insoluble in water, deposited on the outer surfaces of the monolith.

To acquire quantitative information on the sulfate salts formed on the spent catalyst, ion chromatography and ICP-MS experiments were performed on the supernatant solutions obtained by immersing samples of fresh, aged, and thermally regenerated catalysts in water.

In agreement with elemental analysis and SO_2-TPD experiments, it was found that some soluble sulfate species were present on the surface of the virgin catalyst, accounting for roughly 0.5% of its original weight. Moreover, no other anions were detected in significant concentration, thus excluding, in particular, the deposition of ammonium nitrates on the catalyst during its operation in the SCR unit at low temperature. As shown in Table 4, the quantity of soluble sulfates increases for the reaction-aged catalyst reaching 3% of the catalyst weight.

Table 4. Ion chromatography analysis showing the concentration of main anions in the supernatant water after washing samples of the fresh, reaction-aged, and thermally regenerated (R400) SCR catalyst. Results converted to weight% with respect to the catalyst sample.

	F	Cl	NO_3 % wt	PO_4	SO_4
Fresh Catalyst	0.00	0.00	0.00	0.01	0.53
Aged 18 kh	0.00	0.00	0.00	0.01	3.00
Regen. R400	0.00	0.00	0.00	0.00	1.92

The ICP-MS analysis of metal ions in the supernatant water revealed the presence of a significant lower concentration of dissolved calcium (about 0.005% wt.) with respect to the sulfates and the dissolution of a modest amount of vanadium (0.022% of the catalyst weight, corresponding to ca. 0.9% of the original vanadium loading).

Thermal treatment of the aged catalyst at 400 °C reduced the amount of water-soluble sulfates to ca. 1.9% wt. (Table 4), that was still higher than the original value measured for the virgin catalyst.

The effect of the regeneration treatments was further investigated by carrying out TG-MS experiments under N_2 flow either on fresh and aged catalysts as well as on reference sulfate salts. In Figure 6 the weight loss associated with the decomposition of surface salts is compared for the reaction-aged and regenerated catalysts. The aged catalyst showed a well detectable weight loss from roughly 300 °C whereas both regenerated catalysts experienced only a small weight change in the range of temperature investigated. In particular, the water washed catalyst (WW) showed a weak weight loss due to some residual water adsorbed on the surface, whereas the catalyst that was thermally regenerated at 400 °C (R400) displayed a small unexpected weight increase up to 400 °C and thereafter it approached the same final weight.

The inset graph in Figure 6 shows the decomposition of bulk $(NH_4)_2SO_4$ takes place between 260 °C and 460 °C with a characteristic two-step process resembling the trend of weight loss observed for the aged catalyst in the same temperature range. In order to further confirm this hypothesis, the TG analysis was also performed on a sample of the fresh catalyst to which 10 wt% of $(NH_4)_2SO_4$ was added by impregnation (with a water solution) followed by drying at 120 °C. As shown in Figure 6, the weight loss followed the same qualitative trend observed for the aged catalyst. Therefore, it can be argued that ammonium sulfate was one of the main species accumulated on the catalyst during 18 kh of SCR operation at low temperature. Its total amount on the catalyst accounted for a maximum of 1–1.5% wt. and it could be removed by either thermal regeneration treatments at temperatures above 400 °C or by washing with water.

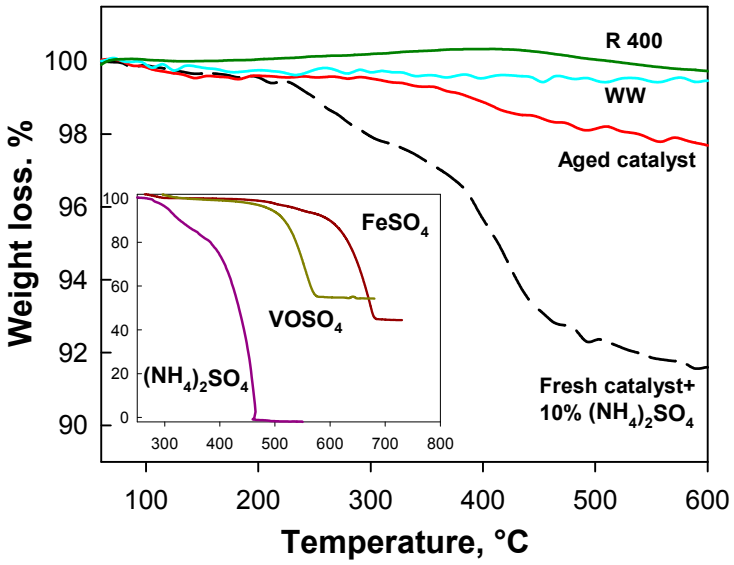

Figure 6. TG analysis (in N_2) of a fresh catalyst sample impregnated with 10 wt% $(NH_4)_2SO_4$, a reaction-aged catalyst sample, and the same catalyst after regeneration by either thermal treatment (R400) or water treatment (WW). The inset shows the TG profile recorded for the thermal decomposition of reference bulk sulfates.

Accordingly, the MS profile of SO_2 (m/z = 64) that evolved from the reaction-aged catalyst (Figure 7) revealed a main emission peak at about 410 °C followed by a long tail extending up to 850 °C with poorly resolved, low-intensity peaks at ca. 550 and 750 °C. By comparison with the SO_2 profile obtained from the fresh catalyst sample impregnated with 10% $(NH_4)_2SO_4$ it can be confirmed that decomposition of ammonium (bi) sulfate was responsible for the first emission peak around 400 °C. In agreement with the results of elemental analysis showing (Tables 1 and 4) some different sulfate species were already present on the fresh catalyst, it can be inferred that those sulfates that bonded to titania, $VOSO_4$, and iron sulfates, contributed to SO_2 emission in the temperature range from 400 °C to 800 °C. On the other hand, $CaSO_4$ deposits, whose presence on the surface of the aged catalyst was detected by SEM-EDS analysis, would require higher temperatures (in excess of 900 °C) to start decomposing under flowing N_2.

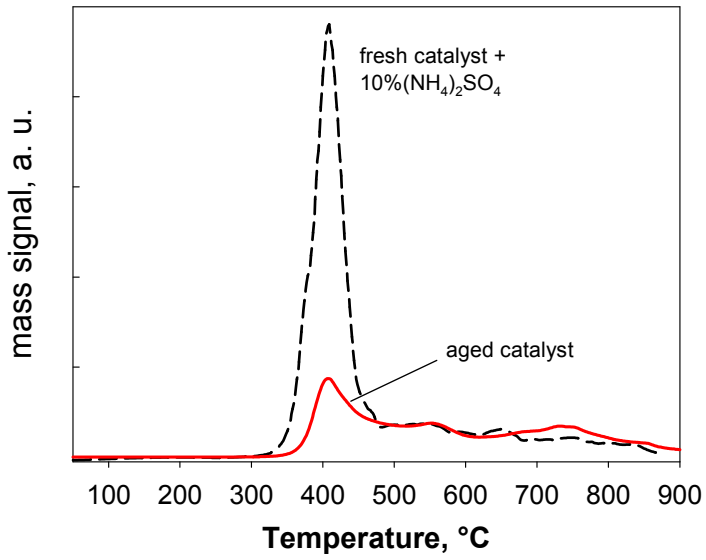

Figure 7. MS profiles of SO_2 (m/z = 64) recorded during the TG analysis (Figure 6) of the fresh catalyst sample impregnated with 10 wt% $(NH_4)_2SO_4$ and the 18 kh reaction-aged catalyst.

The absence SO_2 signals at high temperature for WW regenerated catalyst indicates that $CaSO_4$ deposits were detached and/or partly solubilized in water: indeed, a bulk solubility of 2.4 g/L at room temperature [25] is large enough to assure dissolution of small $CaSO_4$ surface particles.

This conclusion explains the reason why WW regeneration is more effective than thermal regeneration. In fact, the thermal treatment could only promote ammonium sulfate decomposition, which largely occurs at T < 400 °C, as also reported by Gan et al. [26], whereas WW solubilized also the other more stable sulfates and easily removed ash debris poorly attached to the monolith walls. This result is roughly in agreement with data reported in Table 4 showing that only 1/3 of the total sulfates were removed through thermal regeneration, whereas with the washing treatment it was possible to remove the remaining fraction.

In Figure 8, the FTIR spectra of the fresh, aged and regenerated catalysts are reported. The fresh catalyst showed, in addition to the small band at 980 cm^{-1} assignable to both hydrated vanadyl and wolframyl groups [16], also a large broad band consisting of overlapping signals with maxima at about 1135 and 1050 cm^{-1} attributed to bi-dentate sulfate on TiO_2 [16,27]. Sulfation of the TiO_2 support in the fresh sample was already deduced by elemental analysis and TPD-SO_2 results and it is deliberately performed to enhance the intrinsic SCR activity by increasing the number of Brønsted acid sites [17]. Aging under reaction for 18 kh caused the appearance of an additional sharp band at about 1400 cm^{-1}, a shoulder at about 1210 cm^{-1}, and a slight increase in the intensity of the band at 1050 cm^{-1}. These two last bands are related to further TiO_2 sulfation [16,26,27]. Moreover, the 1400 cm^{-1} band, detected in sulfated V_2O_5/TiO_2 catalysts, is attributed to the asymmetric bending vibrations of NH_4^+ [17,26] although, the superimposition of a band at 1383 cm^{-1}, assigned by Li et al. [11] to $VOSO_4$, cannot be excluded. In order to confirm that ammonium sulfate or bisulfate were present in the aged catalyst, the reference spectrum for the fresh catalyst impregnated with 10% wt. $(NH_4)_2SO_4$ was also recorded and it is reported in Figure 8. In agreement with TG-MS results, similar but more intense signals were found for this reference sample compared to the aged catalyst, thus confirming the deposition of ammonium sulfate and/or bisulfate during SCR operation.

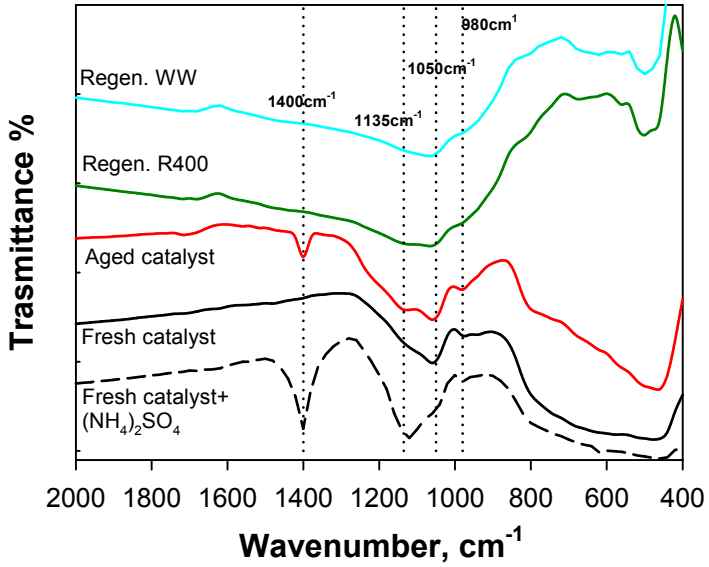

Figure 8. FTIR spectra of the fresh, 18 kh reaction-aged and regenerated (R400 and WW) SCR catalysts as compared to the reference sample of fresh catalyst impregnated with 10 wt% $(NH_4)_2SO_4$.

The absence of the band at 1400 cm^{-1} in the FTIR spectra of regenerated catalysts and the strong reduction of those bands in the range 1000–1230 cm^{-1} indicate that it was possible to (completely) remove those ammonium sulfate deposits by either a thermal treatment at 400 °C or by washing in water. In fact, ammonium sulfates are highly soluble in water and can be thermally decomposed at temperatures around 400–450 °C [27].

Characterization results showed that sulfates were accumulated on the aged catalyst, in spite of the tail end arrangement of the SCR unit guarantees rather low concentrations of SO_x in the inlet feed to the reactor. One possible source is related to the entrainment of small $CaSO_4$ particles escaping the upstream filters. Moreover, it has been reported that sulfation occurs at 200 °C via the weak adsorption of SO_2 molecules on the catalyst (favored at low temperature) as SO_3^{2-} species that are further oxidized by vanadia to form bridged bidentate sulfates bound to titania sites [20]. Thereafter, ammonium (bi) sulfate species deposit on the catalyst through the reaction between adjacent adsorbed NH_3 and sulfate species. In fact, ammonium sulfate and bisulfate are stable at the low operating temperatures (around 200 °C) typical of this SCR unit, whereas the ammonia consumption rate by the SCR reaction is not fast enough to inhibit the formation and accumulation of those compounds, which cover the active sites and plug the pores [5,17,18].

On the other hand, calcium was also found to accumulate on the catalyst, and it can reduce the activity by decreasing of both Lewis and Brønsted sites [9] and/or masking the catalyst surface [5]. However, in the present case, the reaction-aged honeycomb catalyst remained relatively clean as it was exposed to a dust free flue gas. Moreover, Odenbrand [12] noticed, for V_2O_5-WO_3/TiO_2 SCR catalyst utilized in a diesel power plant, that deactivation by $CaSO_4$ in the real system was lower than that simulated by impregnation of the catalyst with $CaSO_4$. They explained this difference supposing that a surface layer of $CaSO_4$ deposits on the catalyst during the use on the engine whereas the impregnation from solution promotes the introduction of calcium sulfate into the pores of the catalyst.

Notably, a relatively high calcium content was detected by EDS analysis on the outer surface of 18 kh aged honeycomb catalyst (particularly close to its inlet section), but the concentration of Ca dissolved in the supernatant solution obtained after washing this sample in water was rather low (well below the solubility of $CaSO_4$). This suggests the presence of poorly soluble species such as $CaCO_3$, that is also possibly formed in the upstream desulfurization unit, or it can be formed in situ together with ammonium sulfates by the reaction of $CaSO_4$ with NH_3 in the presence of CO_2 and water.

2.2. Catalytic Testing

Results of catalytic tests on fresh, aged, and regenerated catalysts are shown in Figure 9a–d. The NO conversion profile as a function of temperature showed a typical broad maximum in the range between 300–400 °C (Figure 9a). At higher temperatures, the direct ammonia oxidation reaction started to proceed at significant rates consuming the reactant for the SCR reaction of NO while also leading to the formation of different nitrogen oxides (including NO) apart from N_2, thus apparently decreasing NO conversion. Accordingly, ammonia conversion increased monotonically along with the reaction temperature approaching 100% for T > 300 °C without any further decrease (Figure 9b). In line with many literature reports, the fresh V_2O_5-WO_3/TiO_2 catalyst was very selective towards the formation of N_2 up to 300 °C (Figure 9c), whereas at higher temperatures the selectivity dropped due to the undesired formation of increasing quantities of N_2O in addition to N_2.

A clear reduction of catalytic activity was observed for the aged catalyst used for a total of 18kh in the industrial reactor. Both the NH_3 and NO conversion curves relevant to the aged catalyst sample were generally shifted towards higher temperatures in their ascending brands (Figure 9a,b). A 100% selectivity to N_2 was still measured up to 300 °C (Figure 9c), but, for higher temperatures, the aged catalyst showed a more pronounced tendency to form N_2O.

All regeneration treatments were able to restore most of the original catalytic performance, with a small but still measurable advantage for the washed catalyst.

The kinetic constant for the NO consumption rate and the corresponding apparent activation energy were estimated from integral reactor conversion data under the common assumptions of an ideal isothermal plug flow behavior and a first-order dependency on NO concentration [16,28].

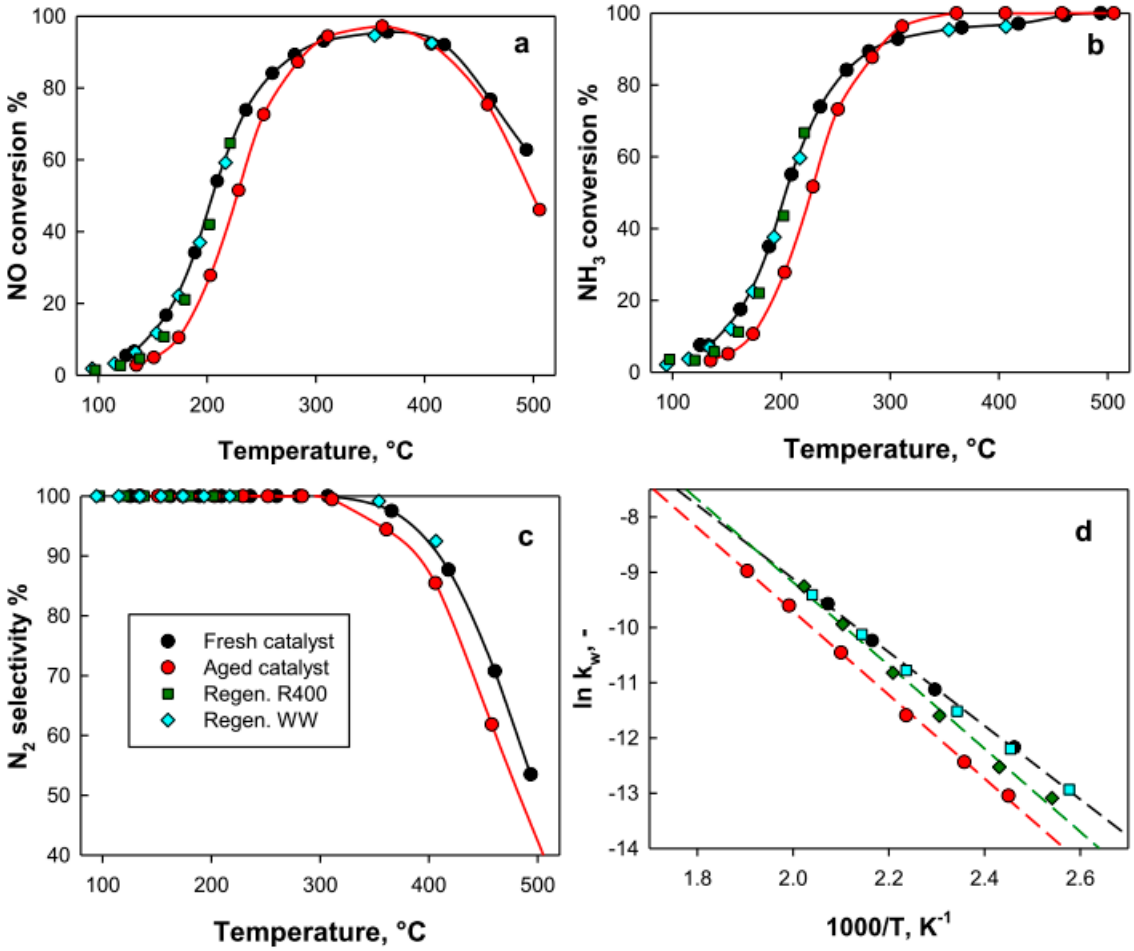

Figure 9. NO (**a**) and NH_3 (**b**) conversion and N_2 selectivity (**c**) as a function of the reaction temperature during the NH_3-SCR tests on fresh, aged, and regenerated (R400 and WW) catalyst; (**d**)) Arrhenius plots showing the corresponding values of the NO reaction rate constant as a function of inverse temperature.

Figure 9d reports Arrenhius plots for the specific (mass-based) NO consumption rates: data sets obtained for each catalyst in the low to mid conversion range showed a linear trend, thus suggesting that they were representative of a predominantly kinetic regime. Apparent activation energy values (E_a) were estimated from the slope of the corresponding Arrhenius plots and are reported in Table 5.

Table 5. Kinetic parameters E_a and $k_w{}^0$, values of the kinetic constant and relative activity at 200 °C for fresh, aged, and regenerated catalysts.

	Ea kJ/mol	ln $k_w{}^0$ $m^3/(g\ s)$	k_w (200 °C) $m^3/(g\ s)$	Relative Activity %
Fresh catalyst	54.3	3.89	5.02E-05	100
Aged 18 kh	63.0	5.44	2.58E-05	51
Regen. R400	62.6	5.88	4.38E-05	87
Regen. WW	54.8	4.00	4.84E-05	96

The fresh catalyst displayed an apparent activation energy equal to 54 kJ/mol, in general agreement with results for analogous systems in the literature [11,17]. Upon aging under SCR conditions, E_a value increased up to 63 kJ/mol, whereas the kinetic constant evaluated at 200 °C decreased by almost 50% from 5.02×10^{-5} to 2.58×10^{-5} $m^3/(g\ s)$ (Table 5). This figure should be regarded as the maximum degree of deactivation experienced by the reaction-aged catalyst after 18 kh of operation since it was calculated for a sample taken from the uppermost inlet section of a honeycomb catalyst module placed

in the first layer of the SCR reactor. It is confirmed that catalyst deactivation proceeded at a relatively low rate due to the tail-end installation of the SCR unit. Nevertheless, an increase of only 10–15 °C in the operating temperature of the SCR reactor was required to compensate for the activity loss due catalyst deactivation has a significant adverse economic impact due to the increased operating costs to re-heat the flue gases exiting the $DeSO_x$ unit and filters [5].

Notably, with the washing treatment in water, it was possible to restore the original value of the apparent activation energy; moreover, the kinetic constant calculated for the regenerated WW catalyst was equal (within experimental error) to that of the fresh system (Table 5). On the other hand, the thermal regeneration at 400 °C was slightly less effective in recovering the catalytic activity at 200 °C, with a calculated kinetic constant equal to 87% of the initial value. However, the thermal treatment was not able to restore the apparent activation energy that remained at 62.6 kJ/mol.

At least two main causes of deactivation were identified on the basis of the characterization of fresh and spent catalyst: ammonium sulfate and/or bisulfate and calcium.

Ammonium bisulfate causes the deactivation of the catalyst at low temperature but it can activate it at a higher temperature (350–450 °C) through sulfation of TiO_2 [6]. In agreement with this assertion, the aged catalyst performed worse than its fresh counterpart up to 300 °C; however, during those SCR tests at higher temperatures, ammonium (bi) sulfates started to be desorbed and decomposed (also by reaction with NO [20]), so that the overall catalytic performance was almost restored.

In addition, alkaline earth metals are reported to deactivate SCR catalysts, although to a lesser extent compared to alkaline metals [13]. In particular, Kröcher and Elesener [13] reported that calcium, as $CaSO_4$, has a poor deactivation effect but if calcium is not or only partly sulfated it has a stronger deactivation potential. They found that calcium does not form vanadates, like potassium, but can deposit on vanadia sites or also on titania or tungsta sites, reducing the ammonia surface coverage acting as a buffer for active sites.

Both types of regeneration treatments mostly removed ammonium sulfates (see spectra in Figure 8). Washing in water caused limited leaching of soluble vanadia species from the catalyst and removed most of its sulfur content. Those effects did not significantly limit the recovery of activity with respect to the virgin catalyst. On the contrary, the residual presence of calcium compounds (sulfates and carbonates) probably limited the effectiveness of the thermal regeneration treatment. In particular, a comparison between the apparent activation energy values for the fresh, aged, and regenerated catalysts suggests that ammonium (bi)sulfate reduced the number of available active catalytic sites for the SCR reaction, whereas Ca compounds induced an additional but limited poisoning effect at low temperature.

3. Materials and Methods

3.1. SCR Catalyst

The industrial V_2O_5-WO_3/TiO_2 SCR catalyst studied in this work was obtained in its virgin form and after a total of 18,000 h of continuous operation for the purification of the exhaust gases of a municipal solid waste to energy plant located in Italy, which adopts a tail-end configuration for the DeNOx unit operating at low temperature [15] after the $DeSO_x$ and Electrostatic precipitation units.

Catalytic elements consisted of extruded honeycomb monoliths (15 cm × 15 cm × 105 cm) with parallel channels with square section. Samples were cut out (length = 3 cm) from the front section (gas inlet) of the original monoliths and, after being eventually ground in an agate mortar, they were subjected to the characterization analyses and catalytic tests.

3.2. Regeneration Procedures

Similar samples (ca. 1 cm × 2 cm × 3 cm) taken from the inlet section of the reaction-aged monolith catalyst were regenerated according to two different procedures: (i) thermal treatment in static air at

400 °C or 450 °C for 2 h; (ii) washing in distilled water (7.5 g of catalyst per cm^3 of water) at room temperature for 30 min (first 15 min in ultra-sound bath) followed by drying in air at 120 °C.

3.3. Physical and Chemical Characterization

The chemical analysis of the catalysts was performed by X-ray fluorescence (XRF) using a Bruker M4 Tornado instrument (Billerica, MA, USA).

Scanning Electron Microscopy (SEM) was performed with a Phenomworld instrument (Eindhoven, The Netherland), equipped with energy dispersion microprobe (EDS) for chemical analysis.

The textural properties were determined by N_2 adsorption at 77 K from p/p_0 10^{-5} using a Quantachrome Autosorb 1-C analyzer (Quantachrome Instruments, Boynton Beach, FL, USA) using the BET method for the calculation of the specific surface area, and the Barrett–Joyner–Halenda (BJH) method applied to the desorption branch for pore size distribution (PSD).

Powder X-ray diffraction (XRD) analysis was performed with a Rigaku Miniflex 600 instrument (Tokyo, Japan) operated with the following acquisition parameters: radiation $Cu_{k\alpha}\lambda$ = 1.54060 nm; range 2θ 3–90°; step 0.02°; time per step 0.1 s.

FT-IR analysis was performed on disks of KBr mixed with 2% wt. of the powdered catalyst sample using a Perkin Elmer Spectrum GX spectrometer (Waltham, MA, USA) equipped with a liquid-N_2 cooled MCT detector, with a spectral resolution of 4 cm^{-1}, averaging each spectrum over 64 scans. All spectra for fresh, aged and regenerated catalysts were ratioed against the spectrum of pure TiO_2 anatase.

Thermo-gravimetric analysis coupled with mass-spectometry (TG-MS) was performed in a Setaram Labsys Evo TGA-DTA-DSC 1600 (Setaram Instrumentation, Caluire, France) flow microbalance connected via a heated capillary to a Pfeiffer Thermostar G mass spectrometer for the analysis of the evolved gases.

Temperature programmed desorption (TPD) of NH_3 or SO_2 was carried out in the same experimental rig used for catalytic activity tests (see below). For each test 125 mg of powdered catalyst was used. In the NH_3-TPD of the fresh catalyst, the sample was initially saturated at 100 °C with a flow of NH_3/He mixture (530 ppmv); thereafter, NH_3 was desorbed by heating at 10 °C/min up to 650 °C under He flow (20 Std dm^3/h). For the NH_3-TPD analysis of the reaction-aged catalyst, ammonia pre-saturation was not performed.

In the case of SO_2-TPD, samples of the virgin or aged catalyst were heated at 10 °C/min up to 1000 °C under N_2 flow while monitoring the SO_2 released due to the decomposition of sulfates present on the catalyst with an UV continuous analyzer (ABB Advanced Optima Limas 11 UV, Zürich, Switzerland).

The concentration of ionic species released from fresh, aged, and regenerated catalyst samples during washing in the aqueous phase was evaluated by means of an 883 Basic IC Plus ionic chromatograph (Metrohm) and an Agilent 7500 ICP-MS. To this aim ca. 50 mg of each catalyst sample were contacted at room temperature with 10 mL of distilled water.

3.4. Selective Catalytic Reduction of NO

The catalytic tests were carried out in a lab-scale fixed bed tubular quartz reactor (10 mm internal diameter) placed in a tubular furnace and operated in the temperature range 90–550 °C as described in [14,29], using 0.125 mg of powdered catalyst (125–200 μm particle diameter).

High-purity gas streams (NO in He, NH_3 in He, O_2, He) from cylinders were regulated by four independent mass flow controllers (BROOKS MFC SLA5850S) and mixed at nearly atmospheric pressure before entering the reactor at a total flow rate of 25 Std dm^3/h, corresponding to a gas hourly space velocity of 100,000 h^{-1}. The feed composition was NO = NH_3= 400 ppmv (NO_2 impurity < 4 ppmv), 6% O_2 balanced with He.

Gas analysis was performed by two continuous analyzers with independent detectors respectively for (i) NH_3 (Tunable Diode Laser Spectroscopy, GAS 3000R Geit-Europe); (ii) NO, N_2O (ND-IR) and

NO_2 (UV) (Emerson X-Stream XEGP). A Sycapent™ (P_2O_5) trap was used to remove water and NH_3 from the gas stream before entering the NOx analyzer. N_2 concentration in the products was estimated by N-balance (excluding the eventual formation of other N-bearing species apart from those measured). NH_3 and NO conversions and N_2 selectivity were calculated as defined in [14].

4. Conclusions

The deactivation of a commercial V_2O_5-WO_3/TiO_2 honeycomb catalyst operated 18,000 h in a tail-end selective catalytic reduction De-NOx unit treating the exhaust gases from a MW incinerator in Southern Italy was investigated as a case study. The SCR catalyst generally operated at around 200 °C with a relatively clean inlet feed after a desulphurization unit with CaO/CaOH and fabric filters. Nevertheless, catalyst deactivation was observed to cause as much as a 50% reduction in the rate of reaction evaluated at 200 °C (worst scenario).

Results of the characterization of fresh and spent catalyst suggested at least two main causes of deactivation: The formation of ammonium sulfate and/or bisulfate and the deposition of calcium sulfate. The former species slowly formed through the reaction between adjacent adsorbed NH_3 and sulfate species; the latter was related to the entrainment of small $CaSO_4$ particles escaping the filters located upstream the SCR unit.

The effect of ammonium (bi) sulfate was the reduction of the number of available active catalytic sites for the SCR reaction, whereas Ca compounds induced an additional but limited poisoning effect at low temperature, inducing a small increase in the apparent activation energy of the SCR reaction of NO.

Furthermore, laboratory catalyst regeneration studies were carried out comparing the effectiveness to restore DeNOx-activity of thermal treatment in air at 400/450 °C or washing in water at room temperature. Both regeneration treatments were able to remove ammonium (bi) sulfate from the aged catalyst, which was identified as the main cause of deactivation. A residual presence of calcium compounds (sulfates/carbonates) was deduced only in the case of thermally regenerated samples. As a consequence, by washing the aged catalyst in water it was possible to almost completely recover its original SCR activity at low temperature, in spite of a negligible loss of active vanadium species due to solubilization. On the other hand, the thermally regenerated catalyst recovered 87% of the original rate of SCR at 200 °C, although the corresponding value of the apparent activation energy remained close to that measured for the aged catalyst, i.e., 10–15% higher than for the virgin catalyst.

Author Contributions: Data curation, S.C., C.F. and L.L.; investigation, S.C., C.F., and L.L.; supervision, R.C., G.P., S.C. and L.L.; writing – original draft, S.C. and L.L.; writing – review and editing, S.C.

Funding: This research received no external funding

Acknowledgments: Ing. S. Malvezzi (A2A) is kindly acknowledged for providing catalyst samples and valuable support throughout the project.

Conflicts of Interest: The authors declare no conflict of interest.

References

1. Zhang, J.; Li, X.; Chen, P.; Zhu, B. Research Status and Prospect on Vanadium-Based Catalysts for NH_3-SCR Denitration. *Materials* **2018**, *11*, 1632. [CrossRef] [PubMed]
2. Mladenović, M.; Paprika, M.; Marinković, A. Denitrification techniques for biomass combustion. *Renew. Sustain. Energy Rev.* **2018**, *82*, 3350–3364. [CrossRef]
3. Kuo, J.-H.; Lin, C.-L.; Chen, J.-C.; Tseng, H.-H.; Wey, M.-Y. Emission of carbon dioxide in municipal solid waste incineration in Taiwan: A comparison with thermal power plants. *Int. J. Greenh. Gas Control* **2011**, *5*, 889–898. [CrossRef]
4. Yan, Q.; Yang, R.; Zhang, Y.; Umar, A.; Huang, Z.; Wang, Q. A Comprehensive Review on Selective Catalytic Reduction Catalysts for NOx Emission Abatement from Municipal Solid Waste Incinerators. *Environ. Prog. Sustain. Energy* **2016**, *35*, 1061–1069. [CrossRef]

5. Argyle, M.; Bartholomew, C. Heterogeneous Catalyst Deactivation and Regeneration: A Review. *Catalysts* **2015**, *5*, 145–269. [CrossRef]
6. Brandin JG, M.; Odenbrand, C.U.I. Deactivation and Characterization of SCR Catalysts Used in Municipal Waste Incineration Applications. *Catal. Lett.* **2018**, *148*, 312–327. [CrossRef]
7. Brandin JG, M.; Odenbrand, C.U.I. Poisoning of SCR Catalysts used in Municipal Waste Incineration Applications. *Top. Catal.* **2017**, *60*, 1306–1316. [CrossRef]
8. Lisi, L.; Lasorella, G.; Malloggi, S.; Russo, G. Single and combined deactivating effect of alkali metals and HCl on commercial SCR catalysts. *Appl. Catal. B Environ.* **2004**, *50*, 251–258. [CrossRef]
9. Nicosia, D.; Czekaj, I.; Kröcher, O. Chemical deactivation of $V_2O_5/WO_3–TiO_2$ SCR catalysts by additives and impurities from fuels, lubrication oils and urea solution Part II. *Characterization study of the effect of alkali and alkaline earth metals Appl. Catal. B Environ.* **2008**, *77*, 228–236.
10. Nicosia, D.; Elsener, M.; Kröcher, O.; Jansohn, P. Basic investigation of the chemical deactivation of V_2O_5/WO_3-TiO_2 SCR catalysts by potassium, calcium, and phosphate. *Top. Catal.* **2007**, *42–43*, 333–336. [CrossRef]
11. Li, C.; Shen, M.; Wang, J.; Wang, J.; Zhai, Y. New Insights into the Role of WO_3 in Improved Activity and Ammonium Bisulfate Resistance for NO Reduction with NH_3 over V−W/Ce/Ti Catalyst. *Ind. Eng. Chem. Res.* **2018**, *57*, 8424–8435. [CrossRef]
12. Odenbrand, C.U.I. $CaSO_4$ deactivated V_2O_5-WO_3/TiO_2 SCR catalyst for a diesel power plant. Characterization and simulation of the kinetics of the SCR reactions. *Appl. Catal. B Environ.* **2018**, *234*, 365–377. [CrossRef]
13. Kröcher, O.; Elesener, M. Chemical deactivation of $V_2O_5/WO_3–TiO_2$ SCR catalysts by additives and impurities from fuels, lubrication oils, and urea solution I. Catalytic studies. *Appl. Catal. B Environ.* **2008**, *75*, 215–227. [CrossRef]
14. Cimino, S.; Totarella, G.; Tortorelli, M.; Lisi, L. Combined poisoning effect of K^+ and its counter-ion (Cl^- or NO_3^-) on MnO_x /TiO_2 catalyst during the low temperature NH_3-SCR of NO. *Chem. Eng. J.* **2017**, *330*, 92–101. [CrossRef]
15. a2a Impianti di Termovalorizzazione. Available online: https://www.a2a.eu/it/gruppo/i-nostri-impianti/termovalorizzatori/acerra (accessed on 16 May 2019).
16. Forzatti, P. Present status and perspectives in de-NO*x* SCR catalysis. *Appl. Catal. A Gen.* **2001**, *222*, 221–236. [CrossRef]
17. Guo, X.; Bartholomew, C.; Hecker, W.; Baxter, L.L. Effects of sulfate species on V_2O_5/TiO_2 SCR catalysts in coal and biomass-fired systems. *Appl. Catal. B Environ.* **2009**, *92*, 30–40. [CrossRef]
18. Guo, K.; Fan, G.; Gu, D.; Yu, S.; Ma, K.; Liu, A.; Tan, W.; Wang, J.; Du, X.; Zou, W.; et al. Pore Size Expansion Accelerates Ammonium Bisulfate Decomposition for Improved Sulfur Resistance in Low-Temperature NH_3-SCR. *ACS Appl. Mater. Interf.* **2019**, *11*, 4900–4907. [CrossRef] [PubMed]
19. Wu, G.; Li, J.; Fang, Z.; Lan, L.; Wang, R.; Gong, M.; Chen, Y. $FeVO_4$ nanorods supported TiO_2 as a superior catalyst for NH3–SCR reaction in a broad temperature range. *Catal. Commun.* **2015**, *64*, 75–79. [CrossRef]
20. Li, C.; Shen, M.; Yu, T.; Wang, J.; Wang, J.; Zhai, Y. The mechanism of ammonium bisulfate formation and decomposition over V/WTi catalysts for NH_3-selective catalytic reduction at various temperatures. *Phys. Chem. Chem. Phys.* **2017**, *19*, 15194–15206. [CrossRef]
21. Zhu, Y.; Hou, Q.; Shreka, M.; Yuan, L.; Zhou, S.; Feng, Y.; Xia, C. Ammonium-Salt Formation and Catalyst Deactivation in the SCR System for a Marine Diesel Engine. *Catalysts* **2018**, *9*, 21. [CrossRef]
22. Zhang, Y.S.; Li, C.; Wang, C.; Yu, J.; Xu, G.; Zhang, Z.G.; Yang, Y. Pilot-Scale Test of a V_2O_5-WO_3/TiO_2-Coated Type of Honeycomb DeNOx Catalyst and Its Deactivation Mechanism. *Ind. Eng. Chem. Res.* **2019**, *58*, 828–835. [CrossRef]
23. Saur, O. The structure and stability of sulfated alumina and titania. *J. Catal.* **1986**, *99*, 104–110. [CrossRef]
24. Kanari, N.; Menad, N.-E.; Ostrosi, E.; Shallari, S.; Diot, F.; Allain, E.; Yvon, J. Thermal Behavior of Hydrated Iron Sulfate in Various Atmospheres. *Metals* **2018**, *8*, 1084. [CrossRef]
25. Partridge, E.P.; White, A.H. The Solubility of Calcium Sulfate From 0 to 200°. *J. Am. Chem. Soc.* **1929**, *51*, 360–370. [CrossRef]
26. Gan, L.; Guo, F.; Yu, J.; Xu, G. Improved Low-Temperature Activity of V_2O_5-WO_3/TiO_2 for Denitration Using Different Vanadium Precursors. *Catalysts* **2016**, *6*, 25. [CrossRef]

27. Ye, D.; Qu, R.; Song, H.; Zheng, C.; Gao, X.; Luo, Z. Investigation of the promotion effect of WO3 on the decomposition and reactivity of NH_4HSO_4 with NO on V_2O_5–WO_3/TiO_2 SCR catalysts. *RSC Adv.* **2016**, *6*, 55584–55592. [CrossRef]
28. Dumesic, J.A.; Topsoe, N.-Y.; Topsoe, H.; Slabiak, T. Kinetics of Selective Catalytic Reduction of Nitric Oxide by Ammonia over Vanadia/Titania. *J. Catal.* **1996**, *163*, 409–417. [CrossRef]
29. Gargiulo, N.; Caputo, D.; Totarella, G.; Lisi, L.; Cimino, S. Me-ZSM-5 monolith foams for the NH_3 -SCR of NO. *Catal. Today* **2018**, *304*, 112–118. [CrossRef]